공학석사학위논문

Self-Healable Dielectric PDMS Composite Based on Zinc-Imidazole Coordination Bond

아연-이미다졸 배위결합 기반의 자가치유가능한
유전성 PDMS 복합체

2018 년 8 월

서울대학교 공과대학원
바이오 엔지니어링 협동과정
오 인 영

Abstract

Self-Healable Dielectric PDMS Composite Based on Zinc-Imidazole Coordination Bond

Inyoung Oh

Program of Bioengineering

College of Engineering

Seoul National University

Self-healing material has been intensively studied in the last decade due to its capability of improving material's lifetime and safety. Among the numerous proposed self-healing mechanisms, reversible metal-ligand coordination bond is considered as a strong candidate for a healing moiety because of its high tunability of mechanical properties due to their broad thermodynamics and kinetic parameters. Furthermore, dipolar nature of coordination bond can enhance the dielectric property of the material.

Herein, zinc-imidazole coordination bond, having a fast ligand exchange rate in ambient condition, was employed as a healing moiety to synthesize room temperature self-healable polydimethylsiloxane (PDMS). Imidazole modified acrylate (IMZa) was prepared and imidazole modified PDMS (IMZ-PDMS) was synthesized by grafting IMZa onto PDMS backbone. IMZ-PDMS cross-linked by ligand and zinc ratio 4.5 (IMZ-PDMS-1100 L/Z 4.5) exhibited ultimate tensile strength (U_T) of 60.73 kPa with ultimate extensibility (U_E) of 211.46 %. These mechanical properties could be adjusted by varying L/Z ratio and IMZ content. In comparison with previously reported metal-ligand based self-healing PDMS, IMZ-PDMS-1100 L/Z 4.5 showed faster healing rate that recovered 98 % of U_T and U_E after 31 h healing and even faster healing rate was achieved with higher IMZ content. Moreover, cross-linked IMZ-PDMS displayed high dielectric constant of 8.78 ± 0.42 at 1 MHz, which was 2.9 times higher than conventional PDMS.

Keywords: Self-healing, PDMS, dielectric elastomer, coordination bond

***Student Number*:** 2016-28528

Contents

List of Tables and Figures

1. INTRODUCTION

Biological tissues can maintain their properties and functions for long period of time without external intervention due to their self-healing ability. Unlike biological tissues, most synthetic materials do not have the self-healing ability; therefore, their mechanical properties and functions are decayed over time due to fatigue or damage. Since endowing synthetic materials with the self-healing ability is a promising approach to extend lifespan and safety of the materials, numerous self-healing materials have been proposed.[1] The proposed self-healing materials are classified into extrinsic and intrinsic self-healing based on their healing mechanism. Extrinsic self-healing materials utilize the external healing agents within microcapsules or vascular structure for healing.[2] Once extrinsic self-healing materials are damaged, the healing agent, releasing from the broken the microcapsule or vascular structure, fills the crack and reacts under the presence of a catalyst within the material for healing.[3-5] This extrinsic healing process is generally not repeatable in the healed region because the healing agent is consumed after the first healing. On the other hand, intrinsic self-healing system is inherently able to repair the damage by employing reversible chemical or physical bonds that reconnects the broken linkage

under damage. Hence, self-healing process is repeatable without alteration of material property after healing.[6] In general, reversible covalent bonds and supramolecular interactions were employed as healing moiety for intrinsic self-healing materials. Reversible covalent bonds, such as Diels-Alder reaction and disulfide bond, based healing materials showed relatively strong mechanical properties but their healing processes were often non-autonomous since external energy input was necessary to activate the reversible reactions in most cases.[7-13] In contrast, supramolecular interactions, such as hydrogen bond, host-guest interaction, π-π interaction and metal-ligand coordination, based self-healing materials have autonomous healing process since most of the supramolecular interactions were reversible in an ambient condition.[14-17] Among these supramolecular interactions, metal-ligand coordination bonds offer considerable advantages in controlling mechanical and healing properties through their wide range of thermodynamics and kinetic parameters.[18-19] Unlike hydrogen bonding based self-healing material, metal-ligand coordination bonds are not sensitive to moisture, therefore they are more practical to be applied in industrial fields.[20]

In addition to self-healing ability, introducing metal-ligand coordination bonds into polymer enhance the dielectric property of material due to

dipolar nature of coordination bond.[21-22] Dielectric property indicates the polarizability of material under an electric field. When an electric field is applied to dielectric materials, electron clouds or polar molecules within dielectric materials are shifted against an electric field, causing polarization of material. The polarized dielectric materials can store electric energy temporally thus, the dielectric materials are widely used in electric devices as capacitors. The dielectric elastomer is a type of smart material that is interested in applying to the actuator, energy generator and sensors.[23] However, dielectric elastomers that are currently used in the field have a low dielectric constant (2~3), therefore, they often require high operational voltage or have low sensitivity.[24] In order to reduce the operational voltage and improve its functionality, a dielectric elastomer with a high dielectric constant is demanded.

Previously, several metal-ligand based self-healing polymers that utilized multidentate ligands as healing moieties were reported. However, multiple coordination bonds in the multidentate ligand hinder metal-ligand exchange process; therefore, they required either external stimuli or long healing time for self-healing. For example, Weder et al. proposed a tridentate ligand based self-healing polymer that required UV exposure for healing.[25] Bao et al. suggested bidentate ligand based room temperature self-healable PDMS,

but it took 48 h for 90 % healing of ultimate extensibility.[26] On the other hand, monodentate ligands such as imidazole have only one coordination bond in each ligand, which facilitates the faster ligand exchange than multiple coordination bonds of multidentate ligand. Especially, zinc-imidazole coordination bond was reported to have a fast ligand exchange rate in mild condition.[27] For this reason, zinc-imidazole coordination bond is a promising candidate to achieve fast self-healing rate.

In this study, zinc-imidazole coordination bond was utilized as healing moiety to synthesize room temperature self-healable dielectric PDMS with fast self-healing rate. Influences of IMZa and zinc contents on the mechanical properties of cross-linked IMZ-PDMS were investigated and self-healing tests of IMZ-PDMS with two different IMZa contents were conducted to evaluate the influence of IMZa content on self-healing ability. In addition, dielectric properties of cross-linked IMZ-PDMS were assessed to confirm enhanced dielectric properties due to introducing coordination bond.

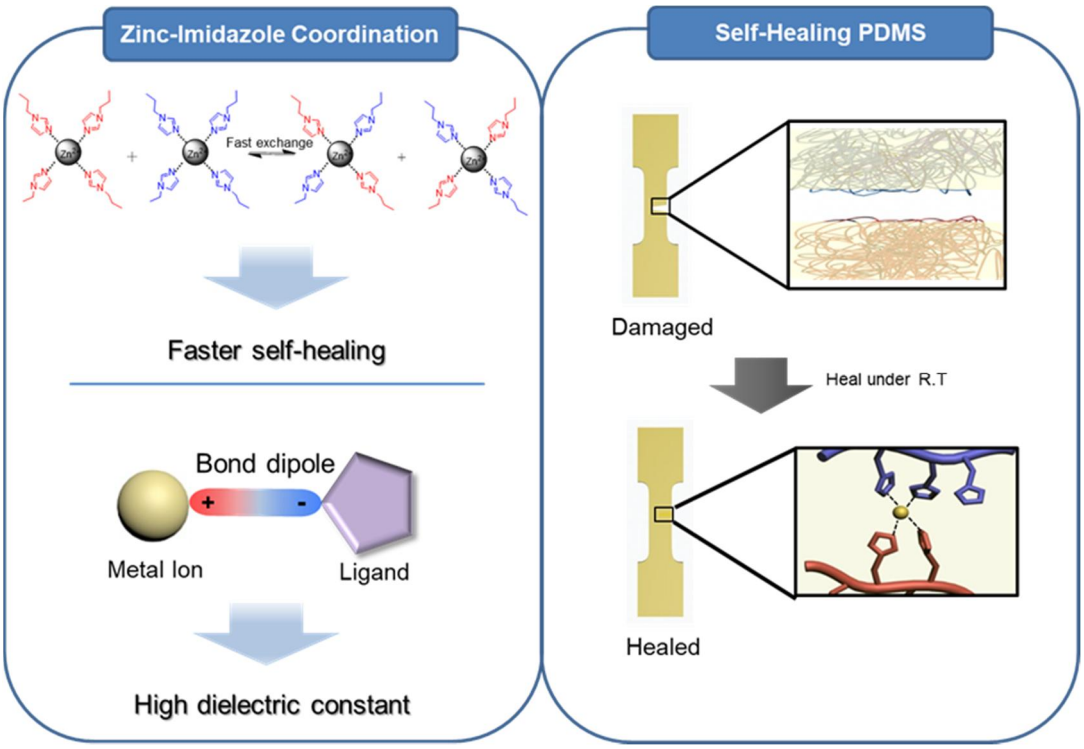

Figure 1. Features of zinc-imidazole based self-healable dielectric PDMS

2. EXPERIMENTS

2.1 Materials

Imidazole (99 %), 1-methylimidazole (99 %), triethylamine (TEA 99 %), acetonitrile (99.5%) were purchased from Sigma Aldrich (St. Louis, USA). 1,4-Bis(acryloyloxy)butane (90 %) was obtained from Tokyo Chemical Industry (Tokyo, Japan). (6-7% Aminopropyl methylsiloxane)-dimethylsiloxane copolymer (AMS-163, M_w 50,000) and (20-25% Aminopropyl methylsiloxane)-dimethyl siloxane copolymer (AMS-1203, M_w 20,000) were purchased from Gelest (Morrisville, USA). Zinc di[bis(trifluoromethylsulfonyl)imide] ($Zn(NTF_2)_2$) (97 %) was purchased from Strem (Newburyport, USA). Dimethylformamide (DMF), tetrahydrofuran (THF) were obtained from Daejung (Siheung, South Korea). All chemicals were used as received without further purification.

2.2 Synthesis of IMZ-PDMS

2.2.1 Synthesis of imidazole modified healing moiety (IMZa)

In a 250 mL 2-neck round bottom flask, 1,4-bis(acryloyloxy)butane (29.1 mL, 146.9 mmol), TEA (5.4 mL, 73.5 mmol), and 1-methylimidazole (1.2 mL, 14.7 mmol) were dissolved in 72.0 mL DMF:CH_3CN mixture (4:5 v/v). The mixture was stirred for 30 min. Imidazole (5.0 g, 73.5 mmol) was dissolved in 13 mL DMF and added dropwise to the mixture for 12 h under N_2 atmosphere. Additional 6 h stirring was allowed to complete the reaction. After the reaction, the solvent was evaporated under *vacuo*. The concentrated light-yellow oil was diluted in ethyl acetate and extracted with brine 5 times to remove TEA, 1-methylimidazole and remaining DMF. The organic layer was dried over magnesium sulfate. Silica flash column chromatography was performed using hexane : ethyl acetate (5 : 5 v/v) to remove unreacted bis(acryloyloxy)butane, and the eluent was gradually switched to ethyl acetate : methanol (95 : 5 v/v) to collect the product. The collected product was kept at 4 ℃ to avoid unwanted polymerization until further use.

^{1}H-NMR ($CDCl_3$, δ, ppm) = 7.44 (s, 1H, Imidazole), 6.97 (s, 1H, Imidazole), 6.87 (s, 1H, Imidazole), 6.36 (d, 1H, C**H$_2$**=CH-C(=O)-), 6.09 (q, 1H, CH_2=C**H**-C(=O)-), 5.78 (d, C**H$_2$**=CH(=O)-), 4.20 (t, 2H, C(=O)-O-C**H$_2$**-CH_2-), 4.10 (m, 4H, -CH_2-C**H$_2$**-O-(O=)C-CH_2-C**H$_2$**-), 2.72 (t, 2H, -O-(O=)C-C**H$_2$**-CH2-), 1.64 (m, 4H, O-CH_2-CH_2-C**H$_2$**-C**H$_2$**-CH2-O-)

2.2.2 Synthesis of IMZa conjugated PDMS. (IMZ-PDMS)

IMZ-PDMS-1100 synthesis: In a 100 mL one neck round bottom flask, AMS-163 (5.0 g, 0.1 mmol) was dissolved using 4 mL THF. IMZa (1.2 g, 4.5 mmol) was dissolved in 1 mL THF and added to the PDMS solution. The mixture was stirred at room temperature for 96 h under N_2 atmosphere and the final product was obtained after evaporating the solvent. In case of IMZ-PDMS-380 synthesis, AMS-1203 (5.0 g, 0.3 mmol) and IMZa (3.3 g, 12.5 mmol) were used as reactant and reaction time was 48 h. Rest of procedures were identical to IMZ-PDMS-1100 synthesis.

^{1}H-NMR ($CDCl_3$, δ, ppm) = 7.50 (s, 1H, Imidazole), 7.04 (s, 1H, Imidazole), 6.93 (s, 1H, Imidazole), 4.26 (t, 2H, C(=O)-O-C**H$_2$**-CH_2-), 4.09 (m, 4H, -CH_2-C**H$_2$**-O-(O=)C-CH_2-C**H$_2$**-), 2.89 (t, 2H, CH_2-NH-C**H$_2$**-CH_2-) 2.77 (t, 2H, -O-(O=)C-C**H$_2$**-CH2-), 2.59 (t, 2H, -Si-CH_2-CH_2-C**H$_2$**-NH-CH_2-), 2.51 (t, 2H, -NH-CH_2-C**H$_2$**-C(=O)-O-), 2.45 (t, 2H, -Si-CH_2-CH_2-C**H$_2$**-N(-CH2)-CH_2-), 1.67 (m, 4H, O-CH_2-CH_2-C**H$_2$**-C**H$_2$**-CH2-O-), 1.54 (m, 2H -Si-CH_2-C**H$_2$**-CH_2-), 0.50 (t, 2H, CH_2-(O-)Si-C**H$_2$**-CH_2-), 0.08 (s, 24H (IMZ-PDMS-380) or 90H (IMZ-PDMS-1100), C**H$_3$**-Si-C**H$_3$**)

2.2.3. Cross-linking IMZ-PDMS via zinc incorporation

IMZ-PDMS (1 g, 0.005 mmol for IMZ-PDMS-1100, 0.003 mmol for

IMZ-PDMS-380) was dissolved in 20 mL THF and added into a 100 ml one neck round bottom flask. The predetermined amount of Zinc di[bis(trifluoromethylsulfonyl)-imide] based on ligand zinc ratio was dissolved in THF (14.5 mg/mL) and added dropwise to the PDMS solution in the rate of 4 ml/h using a syringe pump. The reaction mixture was stirred overnight and concentrated to 2 ml using a rotary evaporator. The concentrated liquid was transferred to Teflon mold in a dimension of 45 mm length x 15 mm width x 20 mm height and dried at room temperature for 24 h. To ensure complete solvent removal, the PDMS mold was placed in 25 ℃ vacuum oven for 48 h and in 50 ℃ vacuum oven for an additional 48 h. (Figure. 2) The cross-linked PDMS film was carefully peeled off from the mold for further test. The average thickness of the sample was about 1.2 mm.

2.3 Characterization

^{1}H-NMR was taken by an Avance-300 (Bruker, Billerica) at 300 MHz frequency in a chloroform-d solvent. FT-IR spectra were measured by

Tensor27 (Bruker, Billerica) with a wavelength range from 500 to 4000 cm^{-1}.

TGA was performed with Q-50 (TA instrument, New Castle) at a heating rate of 10 ℃/min under N_2 atmosphere. The weight-loss curve and its derivatives were obtained in the range of 30 ℃ to 800 ℃.

2.4 Mechanical Test

IMZ-PDMS sample was prepared by cutting into dogbone shape using a laser cutter and acryl jigs were attached to its grip sections for mechanical support. The dimension of the dogbone sample and acryl jig were illustrated in Figure 4. The tensile tests were performed using Instron 3343 (Instron, Norwood) with a strain rate of 5 mm/min at room temperature. 3 samples were tested for each composition, and Young's modulus was calculated by the initial slope (20 % strain) of the strain-stress curve.

2.5 Self-healing Test

For self-healing test, the dogbone shaped PDMS sample was cut 80% of its gauge section width and the cut surfaces were reattached for 1 min with

light pressure. Samples were healed at 25 ℃ for different durations before the tensile test. Tensile test of the healed sample followed the same procedure as previously described in the mechanical test section. 3 samples were tested for different healing time.

2.6 Measurement of Dielectric Constant

The IMZ-PDMS sample was prepared by cutting into a dimension of 1 cm x 1 cm and copper tapes were used as top and bottom electrodes. To obtain dielectric properties of samples, the capacitance of sample was measured by Agilent E4908A LCR meter (Agilent, Santa Clara) at frequencies ranged from 1 kHz to 1 MHz. The dielectric constant k was calculated from the measured capacitance by

$$k = \frac{Cd}{k_0 A} \quad (1)$$

where C is the capacitance of sample, d is the thickness of the sample, A is an area of electrode and k_0 is permittivity of air (8.854×10^{-12} F/m).

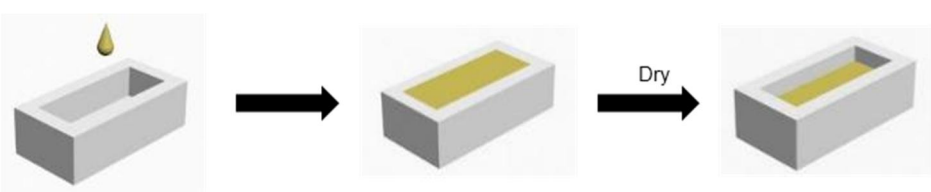

Figure 2. Preparation of IMZ-PDMS sample on Teflon Mold

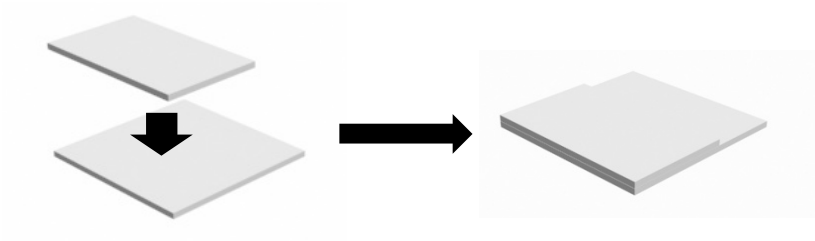

Figure 3. Preparation of acryl jig for mechanical test

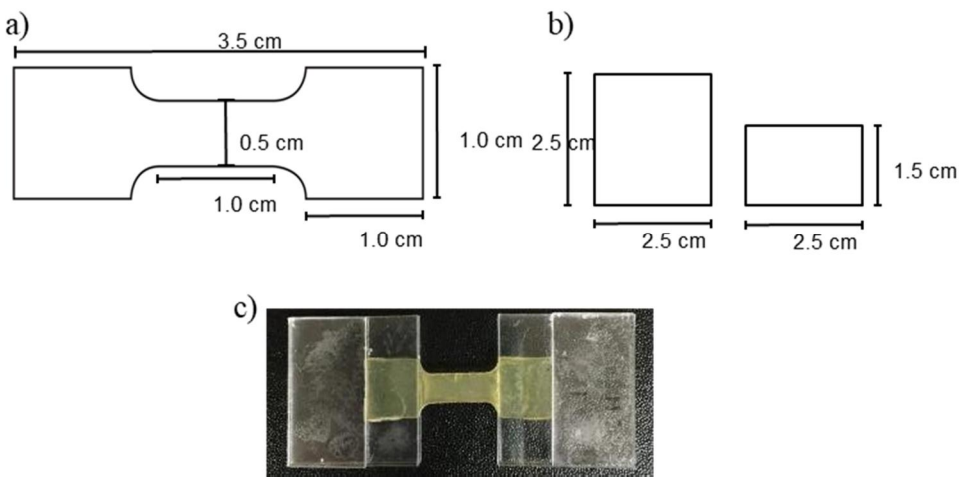

Figure 4. a) Dimension of dog bone sample b) Dimension of jig plates
c) Prepared PDMS sample for mechanical Test

3. RESULTS AND DISCUSSION

3.1 Synthesis and structural characterization

One end of 1,4-bis(acryloyloxy)butane was selectively modified with imidazole via Michael addition reaction in the presence of base catalyst. Synthetic schemes of IMZa and IMZ-PDMS are illustrated in the schemes 1 and 2. For the selective modification of bis(acryloyloxy)butane, 1 equivalent of imidazole was added dropwise into 2 equivalents of 1,4-bis(acryloloxy)butane mixture. After purification using column chromatography, viscous light-yellow oil was obtained with 50 % overall isolation yield. ^{1}H NMR analysis confirmed the complete synthesis of IMZa. As shown in figure 5, the protons of imidazole appeared at 7.46, 7.00 and 6.90 ppm which respectively corresponds to -N-C*H*=N, N-C*H*=CH-, and -CH=C*H*-N-. The integrals of C=C acrylate group protons, which appeared at 6.36, 6.09 and 5.78, were decreased from 2 to 1 as one acrylate group was selectively modified with imidazole.

Synthesized IMZa was grafted on PDMS-NH_2 via Aza-Michael addition. Since the imidazole in IMZa could act as a base catalyst, the reaction was carried without an additional catalyst. Two different PDMS-NH_2 (AMS-163, M_w =50,000 with 6~7 % amine contents and AMS-1203, Mw = 20,000 with

20~25 % amine contents) were used as PDMS backbone to investigate the influence of IMZa contents on mechanical and self-healing properties. IMZ-PDMS-1100 was synthesized using AMS-163 and IMZ-PDMS-380 was prepared from AMS-1203. The numbers after IMZ-PDMS stand for molecular weight between IMZ moieties. The molecular weight of the PDMS backbone, reaction time, and IMZa content for each IMZ-PDMS are summarized in Table 1. Further purification was not required since 100 % IMZa conjugation on PDMS backbone was confirmed by ^{1}H NMR analysis and the viscous light-yellow liquid was obtained as a final product. As shown in Figure 6, proton peaks of acrylate group in IMZa, which were detected at 6.36, 6.09 and 5.78 ppm, completely disappeared and peaks at 2.89, 2.59, 2.53 and 2.43 ppm were observed as new bonds created between acrylate groups of IMZa and amines of PDMS backbone via Michael addition. The FT-IR analysis of IMZ-PDMS also confirmed the complete synthesis of IMZ-PDMS. As shown in figure 7, C=O stretch of the ester group in IMZa was detected at a wavelength of 1734 cm^{-1} in the IMZ-PDMS spectrum while C=O stretch was not observed in the PDMS-NH_2 spectrum.

Linear IMZ-PDMS was cross-linked by zinc ions. $Zn(NTF_2)_2$ was employed as a zinc source because of its good thermal stability and high

mobility of counterion in the solid state. [28] In the absence of zinc ions, IMZ-PDMS was in a viscous liquid phase. However, phase transition occurred from a viscous liquid to an elastomer when zinc salt was added to IMZ-PDMS. In order to confirm that the cross-linking of IMZ-PDMS was based on zinc-imidazole coordination bond, the solubility tests of cross-linked IMZ-PDMS were conducted in THF, chloroform, and ethanol. Before IMZ-PDMS was cross-linked, it was soluble in all of the solvents; however, cross-linked IMZ-PDMS was not soluble in THF and chloroform after 48 h stirring at 50 ℃. On the other hand, ethanol completely dissolved the cross-linked IMZ-PDMS after 48 h stirring at 50 ℃. Considering that ethanol was reported to form a coordination bond with zinc ion, [29] the coordination bond between solvent and zinc replaced the coordination bonds of the zinc-imidazole complex which eventually cleaved the cross-linking points of IMZ-PDMS. This result indicated that that IMZ-PDMS was cross-linked not by chemical bond but zinc-imidazole coordination bond.

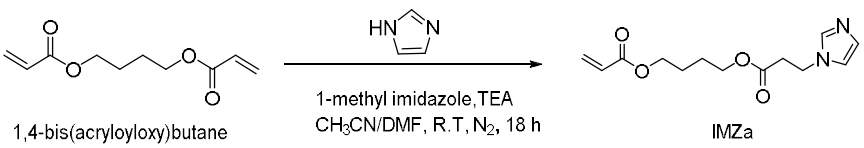

Scheme 1. Synthetic scheme of Imidazole modified acrylate (IMZa)

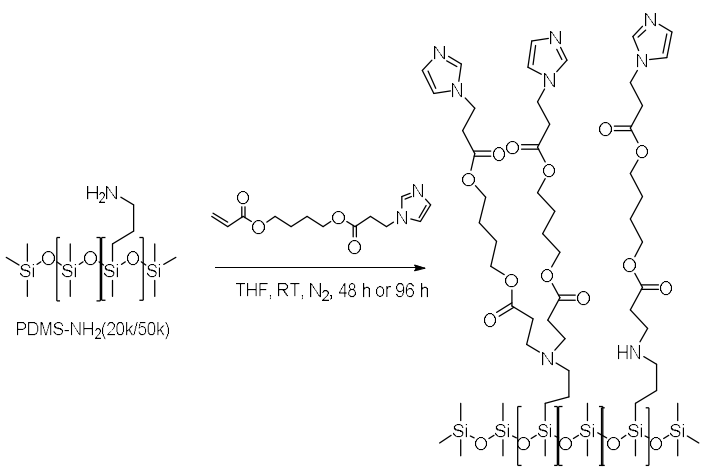

Scheme 2. Synthetic scheme of IMZa conjugated PDMS (IMZ-PDMS)

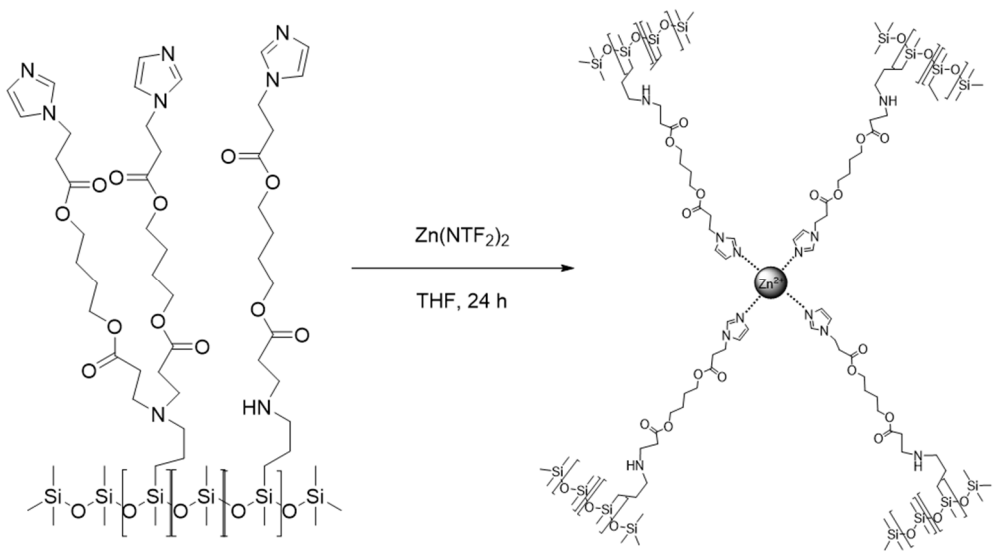

Scheme 3. Synthetic scheme of cross-linked IMZ-PDMS via zinc incorporation

Table 1. Structural characteristics of IMZ-PDMS-1100 and IMZ-PDMS-380

	Backbone M_w (g/mol)	Reaction time (h)	Number of IMZa/chain	IMZa content (mmol/g)
IMZ-PDMS-1100	50,000	96	45	0.89
IMZ-PDMS-380	20,000	48	50	1.55

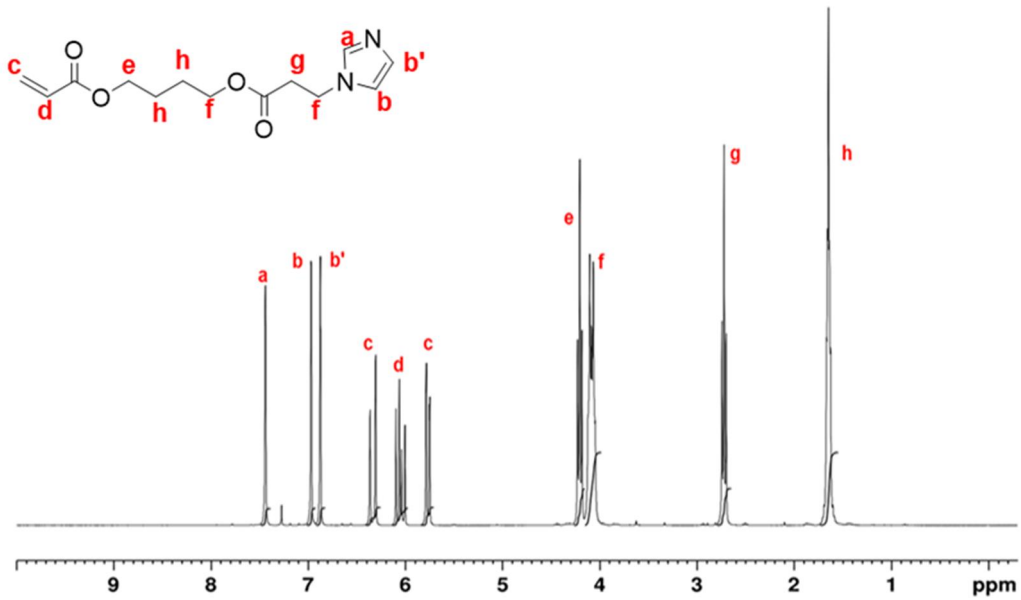

Figure 5. ^{1}H NMR spectrum of IMZa

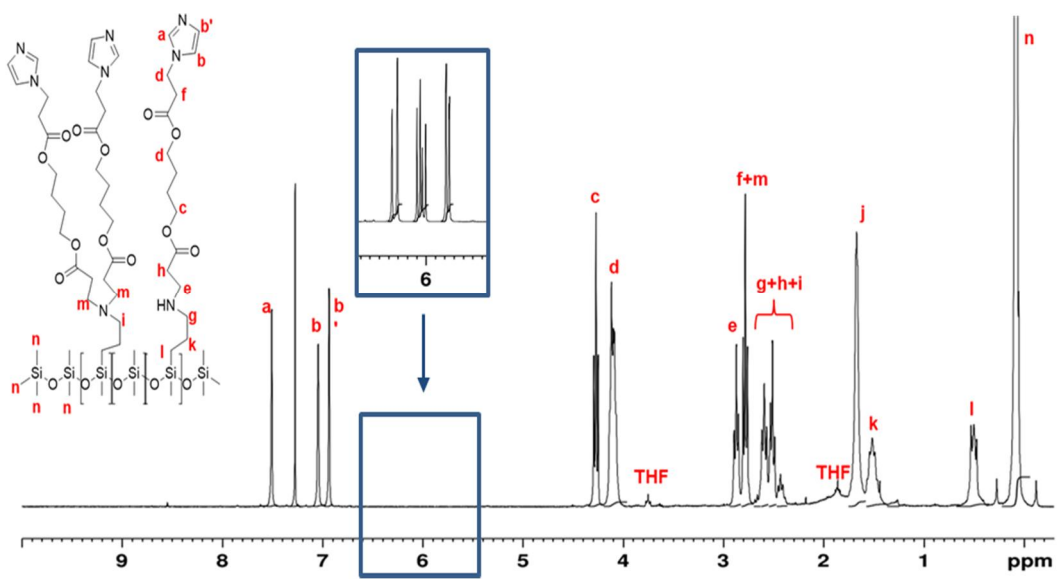

Figure 6. ^{1}H NMR spectrum of IMZ-PDMS

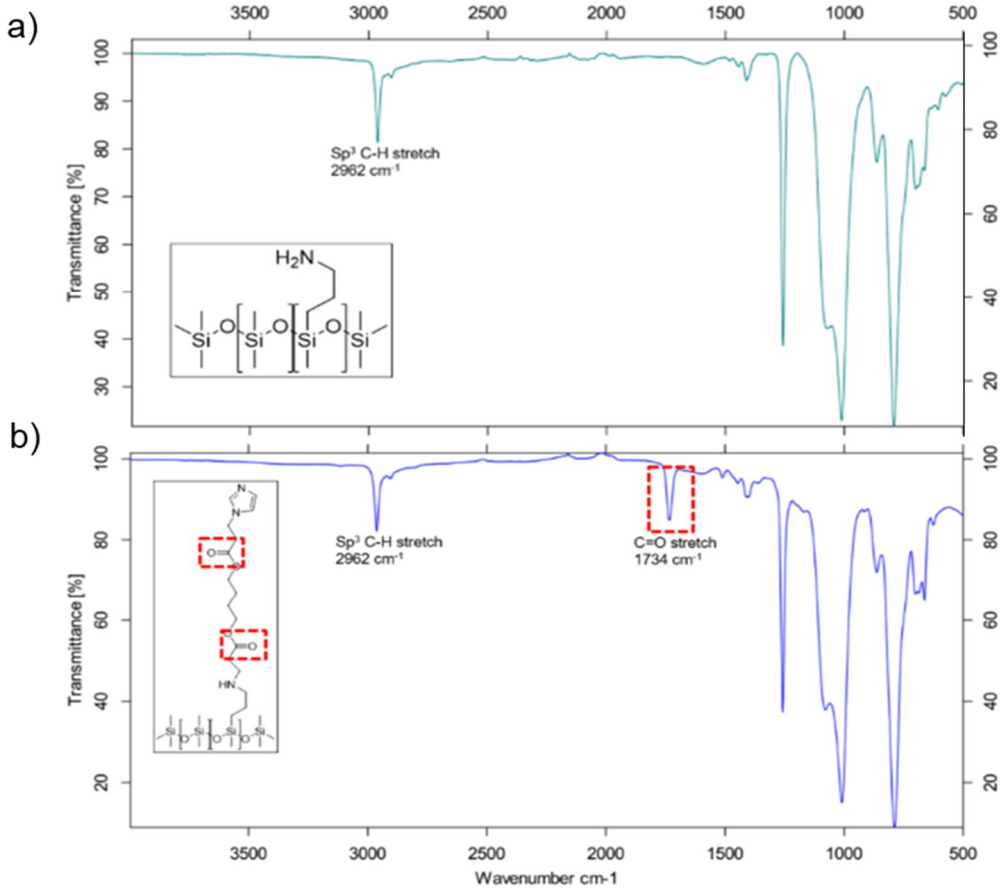

Figure 7. FT-IR spectra of a) PDMS-NH_2 and b) IMZ-PDMS

3.2 Thermal Characterization

Thermal stability of cross-linked IMZ-PDMS was evaluated by TGA measurement. As shown in figure 8a, noticeable weight loss was not observed until 200 ℃ and the initial degradation temperature at 10 wt% loss of original weight (T_{90}) was 283.5 ℃ which indicated that the cross-linked IMZ-PDMS was thermally stable up to 200 ℃. Two degradation stages were observed in the TGA thermogram in which the thermal degradation began at 212.7 ℃ and significant weight loss occurred at 398.0 ℃. The reason for these two degradation stages is that the IMZ healing moiety and PDMS backbone have different degradation temperatures. The ester bond within IMZa moiety displays lower bond dissociation energy (364.1 kJ/mol) compared to that of the Si-O bond (799.6 kJ/mol);[30-31] therefore, degradation of IMZ moiety commenced prior to degradation of PDMS backbone. Total 85.9 wt% of cross-linked IMZ-PDMS was degraded and the remaining mass corresponded to zinc residue.

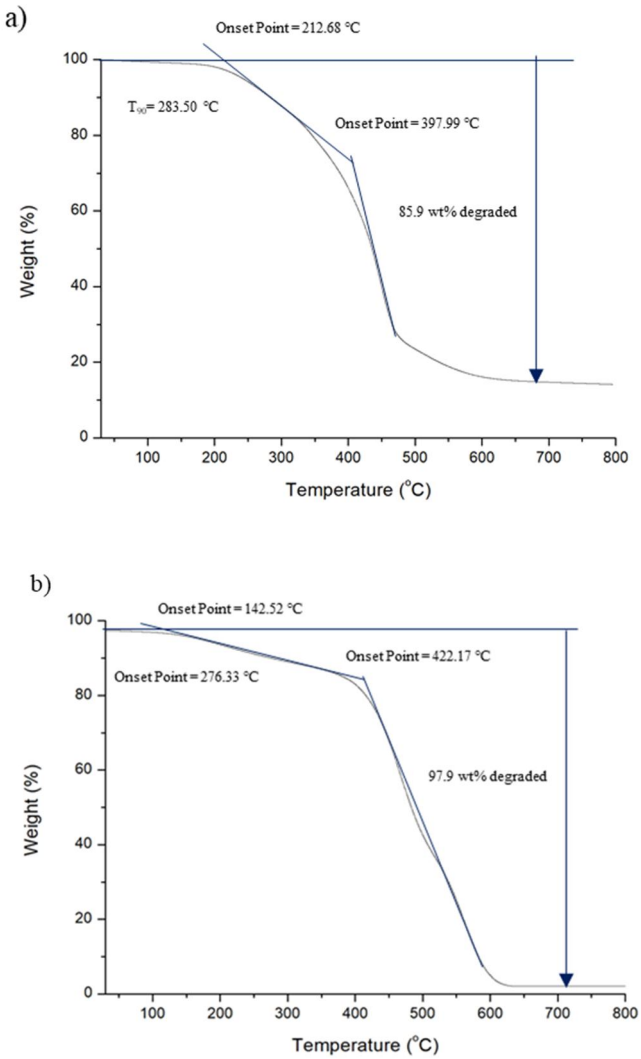

Figure 8. TGA curves for a) cross-linked IMZ-PDMS-1100 L/Z 4.5

b) PDMS-NH_2

3.3 Mechanical Test

Since the zinc-imidazole coordination bond was employed to cross-link linear IMZ-PDMS, the mechanical properties of cross-linked IMZ-PDMS could be tuned by varying IMZ content and ligand zinc ratio. In order to understand the influence of IMZ content on the mechanical property, comparison in the mechanical properties of IMZ-PDMS-1100 and IMZ-PDMS-380 cross-linked by ligand zinc ratio 4.5 were evaluated. As shown in figure 9a, IMZ-PDMS-380 cross-linked by ligand zinc ratio 4.5 (IMZ-PDMS-380 L/Z 4.5) exhibited higher Young's modulus with a value of 115.40 ± 9.13 kPa while Young's modulus of IMZ-PDMS-1100 cross-linked by ligand zinc ratio 4.5 (IMZ-PDMS-380 L/Z 4.5) was 55.45 ± 5.88 kPa. In ultimate extensibility, IMZ-PDMS-1100 L/Z 4.5 showed larger extensibility compare to IMZ-PDMS-380 L/Z 4.5. Considering the fact that higher cross-linking density generally improves the modulus of the material, IMZ-PDMS-380 showed higher Young's modulus due to the higher IMZ content which led to a high cross-linking density.

The ligand zinc ratio also affected the mechanical property of cross-linked IMZ-PDMS. As shown in figure 9b, IMZ-PDMS-1100 L/Z 4 exhibited higher Young's modulus than IMZ-PDMS-1100 L/Z 4.5. In case of ultimate extensibility (U_E), IMZ-PDMS-1100 L/Z 4.5 showed 211.46 ±

10.19 % which was 1.7 folds larger than U_E of IMZ-PDMS-1100 L/Z 4. Mechanical test results of IMZ-PDMS-380 crosslinked by different ligand zinc ratio followed a similar trend with those of IMZ-PDMS-1100. However, this mechanical property change depending on ligand zinc ratio was not only due to cross-linking density but also cross-linking reformation rate. According to Mozhdehi et al, cross-linking reformation rate can be significantly promoted by the substantial amount of uncoordinated ligand which promotes ligand exchange rate.[32] This cross-linking reformation generally relaxes the stress under load but too fast reformation rate at high ligand zinc ratio leads the weaker mechanical property. As ligand zinc ratio approaches to its maximum coordination number (4 in case of zinc ion), the number of uncoordinated imidazole ligands decreases significantly which increases the modulus of the material. Taking into account that IMZ-PDMS-1100 L/Z 4.5 contained uncoordinated imidazole ligand, it showed lower modulus and larger extensibility compare to IMZ-PDMS-1100 L/Z 4.0 in which ligands were fully coordinated. Table 2 summarizes mechanical test results of all compositions.

a)

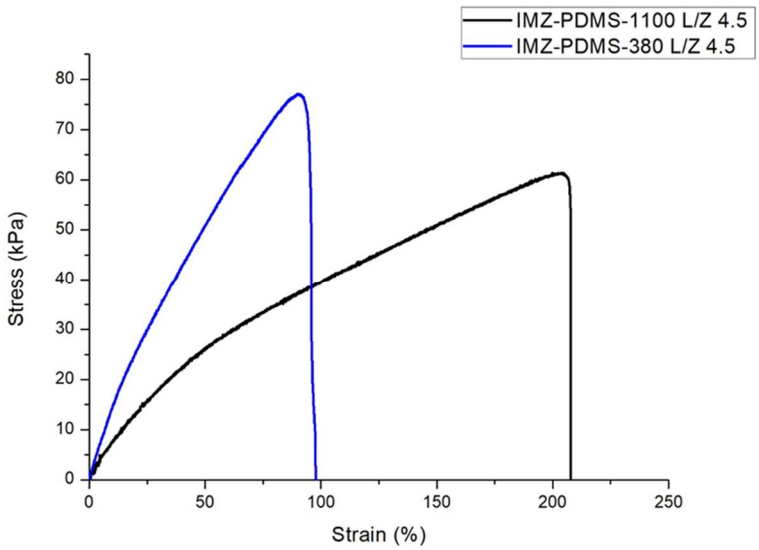

b)

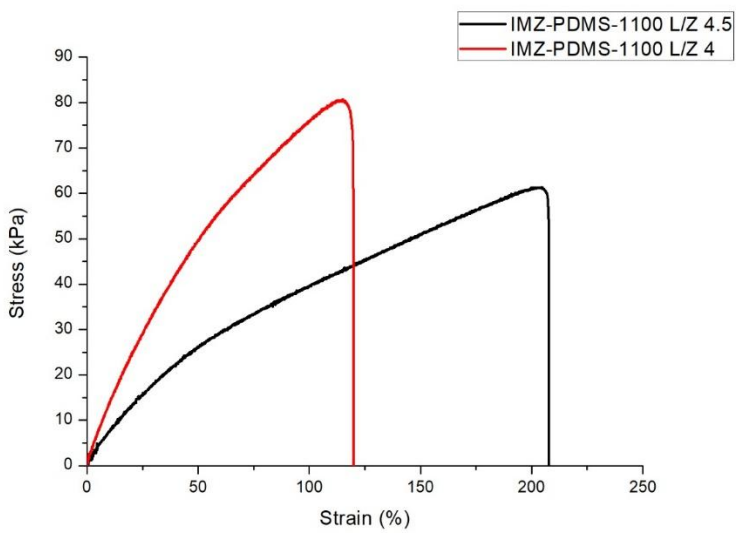

Figure 9. Strain-stress curves of a) IMZ-PDMS-380 L/Z 4.5 vs IMZ-PDMS-1100 L/Z 4.5 b) IMZ-PDMS-1100 with different L/Z ratio

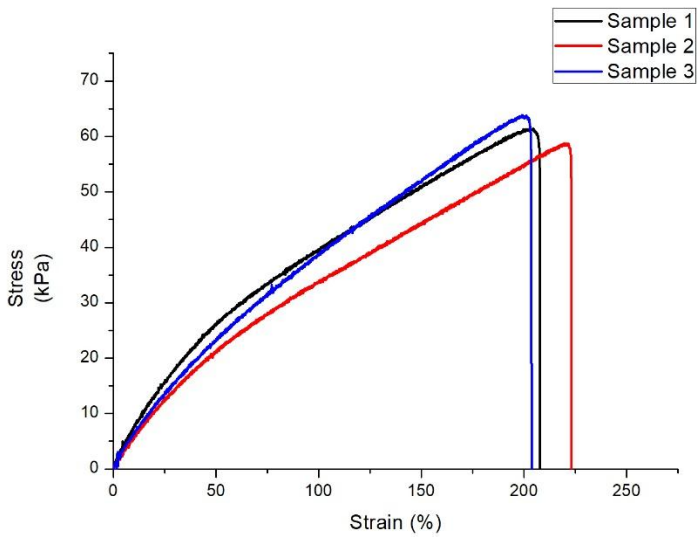

Figure 10. Strain-stress curves of 3 samples of IMZ-PDMS-1100 L/Z 4.5

Table 2. Mechanical test results of IMZ-PDMS (n=3)

	Ultimate Tensile Strength (kPa)	Ultimate Extensibility (%)	Young's Modulus (kPa)
IMZ-PDMS-1100 (4.5 : 1)	60.73± 2.61	211 ± 10	55.45 ± 5.88
IMZ-PDMS-1100 (4 : 1)	75.61 ± 5.31	121 ± 7	110.18 ± 6.81
IMZ-PDMS-380 (4.5 : 1)	73.97 ± 2.59	95 ± 3	115.40 ± 9.13
IMZ-PDMS-380 (4 : 1)	90.12 ± 1.75	70 ± 3	209.18 ± 8.76

3.4 Self-Healing Test

In addition to influence on mechanical properties, the cross-linking reformation underlies the self-healing mechanism of cross-linked IMZ-PDMS. When cut surfaces became in contact, PDMS chains were diffused and stabilized by the cross-linking reformation, leading to the self-healing process of IMZ-PDMS. Since the zinc-imidazole coordination bond showed faster exchange kinetics compared to multidentate ligand based coordination, faster self-healing rate of IMZ-PDMS was expected than that of previously reported multidentate ligand based self-healing PDMS. To investigate self-healing ability of cross-linked IMZ-PDMS, IMZ-PDMS-1100 L/Z 4.5 was selected for self-healing test. Damaged samples were healed at 25 ℃ with different healing time 12, 24, 31h, respectively prior to the tensile test. Figure 11 shows the strain-stress curves of healed samples after different healing time. As expected, IMZ-PDMS-1100 L/Z 4.5 showed higher healing efficiency when longer healing time was allowed. Especially 31 h healing at room temperature led to almost full recovery (higher than 98%) in both U_T and U_E. Table 3 shows all self-healing test results of IMZ-PDMS-1100 L/Z 4.5. On the contrary, previously reported self-healing PDMS, utilizing bipyridine as a healing moiety, required 48 h to heal 90 ± 3% of U_E.

Given that the cross-linking reformation underlies the self-healing

mechanism and it depends on the number of uncoordinated ligands, increasing IMZ content could promote self-healing rate of the cross-linked IMZ-PDMS. To analyze the influence of IMZ content on self-healing ability, additional self-healing test of IMZ-PDMS-380 L/Z 4.5 was performed. As shown in figure 12, IMZ-PDMS-380 L/Z 4.5 showed more than 98 % of U_T and U_E healing efficiencies after only 24 h healing time which was 1.5 times faster than self-healing rate of IMZ-PDMS-1100 L/Z 4.5. Table 4 summarizes the self-healing test result of IMZ-PDMS-380 with L/Z ratio 4.5. These self-healing test results implied that by varying IMZ content, self-healing rate could be promoted along with mechanical properties.

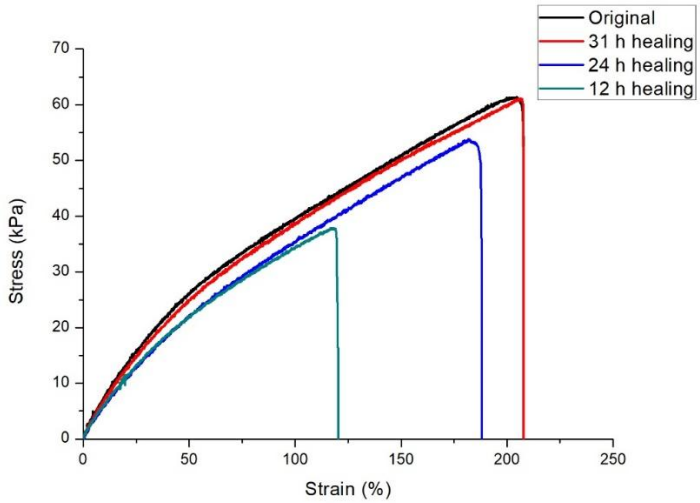

Figure 11. Strain-stress curves of self-healed IMZ-PDMS-1100 L/Z 4.5 after different healing time

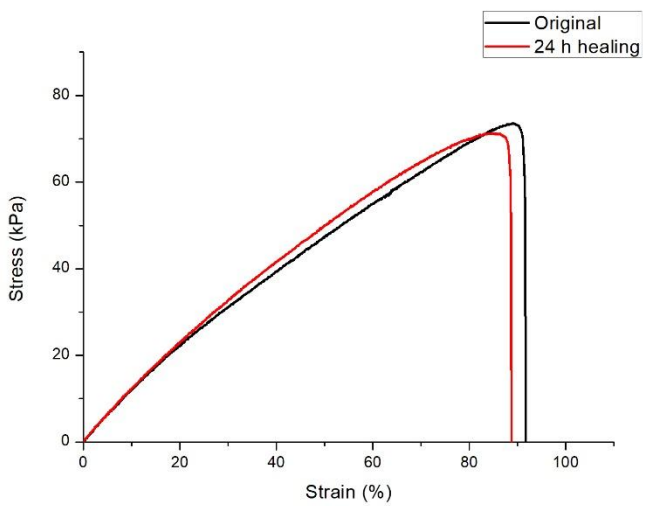

Figure 12. Strain-stress curves of self-healed IMZ-PDMS-380 L/Z 4.5 after 24h healing time

Table 3. Self-healing test results of IMZ-PDMS-1100 L/Z 4.5 (n=3)

	Ultimate Tensile Strength (kPa)	Ultimate Extensibility (%)	U_T[a] Healing Efficiency (%)	U_E[b] Healing Efficiency (%)
Original	60.73 ± 2.61	211 ± 10	-	-
12 h Healed	43.61 ± 5.34	128 ± 10	71 ± 9	58 ± 2
24 h Healed	57.20 ± 1.13	181 ± 8	94 ± 1	86 ± 4
31 h Healed	59.93 ± 2.76	207 ± 9	99 ± 5	98 ± 4

[a] Ultimate Tensile Stress, [b] Ultimate Extensibility

Table 4. Self-healing test results of IMZ-PDMS-380 L/Z 4.5 (n=3)

	Ultimate Tensile Strength (kPa)	Ultimate Extensibility (%)	U_T[a] Healing Efficiency (%)	U_E[b] Healing Efficiency (%)
Original	73.97 ± 2.59	95 ± 3	-	-
24 h Healed	73.16 ± 2.93	92 ± 11	99 ± 4	97 ± 12

[a] Ultimate Tensile Stress, [b] Ultimate Extensibility

3.5 Dielectric Constant Measurement

The dipolar nature of coordination bond enhances the dielectric property of the material. The dielectric constant of IMZ-PDMS was evaluated in order to investigate the enhanced dielectric property of IMZ-PDMS by introducing zinc-imidazole coordination bond. The dielectric constant was calculated using the measured capacitance of IMZ-PDMS by LCR meter. As shown in table 5, IMZ-PDMS exhibited 8.7 ± 0.42 dielectric constant which was 2.90 times higher than the dielectric constant of normal PDMS at 1 MHz. This dielectric constant was also higher than previously reported metal-ligand based dielectric PDMS systems which had 3.2 and 6.4 respectively. Table 6 summarizes mechanical properties, self-healing properties and dielectric properties of IMZ-PDMS and other metal-ligand self-healing PDMS along with conventional PDMS.

Table 5. Dielectric characteristics of IMZ-PDMS-1100 L/Z 4.5 (n=3)

	Freq. (Hz)	1k	10k	100k	1M
IMZ-PDMS-1100 (4.5 : 1)	D.C	19.61 ± 1.55	13.47 ± 0.67	10.82 ± 0.62	8.78 ± 0.42
	D.F	1.04 ± 0.04	0.28 ± 0.01	0.17 ± 0.01	0.13 ± 0.01

Table 6. Mechanical property, self-healing efficiency and dielectric constant of various PDMS

PDMS type	Ultimate Tensile Strength (MPa)	Ultimate Extensibility (%)	Young's Modulus (MPa)	Healing Efficiency[a] (%)	Dielectric Constant (1MHz)	Ref.
PDMS (Sylgard® 184)	3.51~7.65	80 ~ 170	1.32 ~ 2.97	-	2.0~3.0	[33]
H_2PDCA-PDMS	0.23	1860	0.54	90 % (48 h)	6.4	[21]
BPY-PDMS	0.63	340	1.10	90 % (48 h)	3.5	[26]
IMZ-PDMS-1100[b]	0.06	211	0.06	98 % (31 h)	8.7	-

[a] Healing efficiency of ultimate extensibility at 25 ℃ healing [b] IMZ-PDMS-1100 L/Z 4.5

3.6 Possible Application

This high dielectric constant of IMZ-PDMS is desired in capacitive sensor application. Capacitive sensor detects capacitance change when the elastomeric sensor is under deformation and the capacitance of a dielectric elastomer is given by

$$C = k k_0 \frac{A}{d} \quad (2)$$

where k is dielectric constant, k_0 is permittivity of air, A is the area of electrode and d is the thickness of dielectric material. Equation 2 explains that higher dielectric constant yields larger capacitance change under the same change in thickness. Therefore, it is possible to detect capacitance change even in small thickness change if the dielectric constant is high enough. Furthermore, this high dielectric constant enables the miniaturization of the sensor. For this reason, IMZ-PDMS, having high dielectric constant along with self-healing ability,

4. CONCLUSION

Zinc-imidazole coordination bond based self-healable dielectric PDMS was synthesized and its mechanical properties, self-healing ability, and dielectric properties were investigated. Mechanical properties of IMZ-PDMS could be controlled by changing IMZa amount and L/Z ratio. Moreover, IMZ-PDMS displayed good self-healing ability. Comparing with previously reported metal-ligand based self-healing PDMS that required 48 h for 90 % healing of U_E, IMZ-PDMS-1100 with L/Z ratio 4.5 showed faster self-healing rate that required 31 h for 97 % healing of U_E. IMZ-PDMS-380, containing more IMZa content than IMZ-PDMS-1100, with L/Z ratio 4.5 showed even faster healing rate that only required 24 h for 97% healing of U_E. In addition to self-healing ability, the higher dielectric constant was established due to pervasive imidazole-zinc coordination bond within the matrix. Compare to conventional dielectric elastomers and previously reported self-healing dielectric PDMS, IMZ-PDMS-1100 exhibited higher dielectric constant of 8.78 ± 0.43 at 1 MHz frequency which is desired for the dielectric elastomer. In conclusion, we expect that IMZ-PDMS can be a strong candidate as a dielectric elastomer for sensor application with extended lifetime owing to its self-healing capability.

5. REFERENCES

1. S.J. Garcia, *Eur. Polym. J.* **2014,** *53*, 118-125.
2. S.R. White, Sottos, N., Geubelle, P., Moore, J., Kessler, M.R., Sriram, S., Brown, E., Viswanathan, S., *Nature* **2001,** *409* (6822), 794.
3. K.S. Toohey, N.R. Sottos, J.A. Lewis, J.S. Moore, S.R. White, *Nat. Mater.* **2007,** *6* (8), 581.
4. B. Blaiszik, M . Caruso, D. McIlroy, J.S. Moore, S.R. White, N.R. Sottos, *Polymer* **2009,** *50* (4), 990-997.
5. D.Y. Zhu, M.Z. Rong, M.Q. Zhang, *Prog. Polym. Sci.* **2015,** *49-50*, 175-220.
6. Y. Yang, M.W. Urban, *Chem. Soc. Rev.* **2013,** *42* (17), 7446-7467.
7. X. Chen, M.A. Dam, K. Ono, A. Mal, H. Shen, S.R. Nutt, K. Sheran, F. Wudl, *Science* **2002,** *295* (5560), 1698-1702.
8. B.J. Adzima, C.J. Kloxin, C.N. Bowman, *Adv. Mater.* **2010,** *22* (25), 2784-2787.
9. N. Yoshie, M. Watanabe, H. Araki, K. Ishida, *Polym. Degrad. Stab.* **2010,** *95* (5), 826-829.

10. J.A. Yoon, J. Kamada, K. Koynov, J. Mohin, R. Nicolaÿ, Y. Zhang, A.C. Balazs, T. Kowalewski, K. Matyjaszewski, *Macromolecules* **2011,** *45* (1), 142-149.

11. Y. Amamoto, H. Otsuka, A. Takahara, K. Matyjaszewski, *Adv. Mater.* **2012,** *24* (29), 3975-3980.

12. Y. S. Ryu, K. W. Oh, S. H. *Kim, Macromol. Res.,* **2016**, 24(10), 874-880

13. H. Y. Lee, S. H. Cha, *Macromol. Res.,* **2017**, 25(6), 640-647

14. P. Cordier, F. Tournilhac, C. Soulié-Ziakovic, L. Leibler, *Nature* **2008,** *451* (7181), 977.

15. S. Burattini, H.M. Colquhoun, J.D. Fox, D. Friedmann, B.W. Greenland, P.J. Harris, W. Hayes, M.E. Mackay, S.J. Rowan, *Chem. Commun.* **2009,** (44), 6717-6719.

16. A. Zhang, L. Yang, Y. Lin, L. Yan, H. Lu, L. Wang, *J. Appl. Polym. Sci.* **2013,** *129* (5), 2435-2442.

17. N. Roy, E. Buhler, J.M. Lehn, *Polym. Int.* **2014,** *63* (8), 1400-1405.

18. W.C. Yount, D.M. Loveless, S.L. Craig, *J. Am. Chem. Soc.* **2005,** *127* (41), 14488-14496.

19. G.R. Whittell, M.D Hager, U.S. Schubert, I. Manners, *Nat. Mater.* **2011,** *10* (3), 176.

20. D. Mozhdehi, S. Ayala, O.R. Cromwell, Z. Guan, *J. Am. Chem. Soc.* **2014,** *136* (46), 16128-16131.

21. C.-H. Li, C. Wang, C. Keplinger, J.-L. Zuo, L. Jin, Y. Sun, P. Zheng, Y. Cao, F. Lissel, C. Linder, X. You, and Z. Bao, *Nat. Chem.,* **2016**, 6(8), 618.

22. N. Abbas, and H. T. Kim, *Macromol. Res.,* **2016**, 24(12), 1084-1090

23. M. Molberg, Y. Leterrier, C.J. Plummer, C. Walder, C. Löwe, D.M. Opris, F.A. Nüesch, S. Bauer, J.-A.E. Månson, *J. Appl. Phys.* **2009,** *106* (5), 054112.

24. M. Kollosche, H. Stoyanov, S. Laflamme, G. Kofod, *J. Mater. Chem.* **2011,** *21* (23), 8292-8294.

25 M. Burnworth, L. Tang, J.R. Kumpfer, A.J. Duncan, F.L. Beyer, G.L. Fiore, S.J. Rowan, C. Weder, *Nature* **2011,** *472* (7343), 334.

26. Y.-L. Rao, A. Chortos, R. Pfattner, F. Lissel,Y.-C. Chiu, V. Feig, J. Xu, T. Kurosawa, X. Gu, C. Wang, *J. Am. Chem. Soc.* **2016,** *138* (18), 6020-6027.

27. W. Maret, Y. Li, *Chem. Rev.* **2009,** *109* (10), 4682-4707.

28. A. Garcia-Bernabé, V. Compañ, M. I. Burguete, E. García-Verdugo, N. Karbass, S. V. Luis and E. Riande, *J. Phys. Chem. C.* **2010**, 114 (15)

29. B. Li, N. Zimin, M. Vijayakumar, G. Li, J. Liu, V. Sprenkle, and W. Wang, *Nat. Commun.,* **2015***,* 6.

30. L. Raghunanan, and S. S. Narine, *J. Phys. Chem. B,* **2013**, 117(47), 14754-14762

31. Y.-R. Luo, and J. Kerr, *CRC Handbook of Chemistry and Physics,* **2012**, 89, 89.

32. D. Mozhdehi, J. A. Neal, S. C. Grindy, Y. Cordeau, S. Ayala, N. Holten-Andersen, Z. Guan, *Macromolecules,* **2016,** 49 (17), 6310-6321.

33. I. Johnston, D. McCluskey, and C. Tan, M. Tracey, *J. Micromech. Microeng.* **2014**, 24(3).

국문 요약

자가치유물질은 손상이 가해졌을 때 스스로 손상된 부위를 회복할 수 있는 성질을 가진 물질을 총칭한다. 이러한 자가치유물질은 치유방식에 따라서 비본원적(extrinsic), 본원적 치유(intrinsic)로 구분되며, 비본원적 치유는 특정한 자극 없이 치유가 가능하지만 일회적인 치유만 가능하다는 한계점을 가지고 있다. 본 연구에서는 가역적인 금속이온-리간드 배위결합을 이용하여 본원적 자가치유가 가능한 폴리다이메틸실록세인(PDMS)을 합성하였다. 기존 연구에서는 두 자리 또는 세자리 리간드를 이용하여 자가치유물질을 합성하였지만, 여러 자리 리간드와 금속이온의 강한 배위결합력으로 인하여 치유속도가 느린 단점이 보고되었다. 이러한 현상을 감안하여 상온에서 기존연구 보다 빠른 치유속도를 얻기 위해 한자리 리간드인 이미다졸과 아연 사이의 배위결합으로 PDMS을 경화하였으며, 경화된 PDMS는 기존 금속이온-여러 자리 리간드 기반 자가치유 PDMS 보다 약 1.6배 빠른 최대 변형율 회복 속도를 나타냄을 확인하였다. 합성된 자가치유 PDMS는 자가 치유에 이용된 아연과 이미다졸의 쌍극자 결합에 의해 유도되는 분극으로 높은 유전율을 나타내며 LCR 미터로 검증 시 일반적인 PDMS 보다 약 2.9배 높은 유전상수를 나타냄을 확인하였다. 본 연구에서

합성한 자가치유 PDMS는 빠른 자가치유능력과 높은 유전성질을 이용하여 긴 수명을 가지며 높은 민감도를 갖는 변형 및 압력센서로 이용될 수 있을 것으로 기대된다.

주요 어: 자가치유, PDMS, 유전탄성체, 금속-리간드 배위결합

학 번: 2016-28528